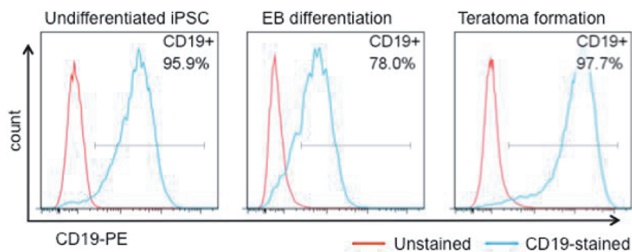


particularly in pluripotent stem cells, limiting their utility for tracking and eventual clinical applications. Targeted integration into genomic “safe harbors” offer a promising alternative approach to mark target cells, potentially circumventing these issues. The adeno-associated virus integration site 1 (AAVS1) has been proposed as a suitable safe harbor for human cells, and we now investigate its utility in our rhesus macaque NHP iPSC model. We have efficiently knocked-in both a truncated CD19 (hΔCD19) marker gene a non-immunogenic and clinical relevant marker, or green fluorescent protein (GFP) at the homologous AAVS1 site in rhesus iPSCs (RhiPSCs) using the clustered regularly interspaced short palindromic repeats/CRISPR-associated nuclease 9 (CRISPR-Cas9) system. PCR and Southern blot analyses demonstrated highly efficient knock-in into the AAVS1 locus, with over one third of clones screened containing only targeted but not random integrations. (Table 1). Edited RhiPSC-GFP/hΔCD19 clones retained a normal karyotype and pluripotency - as shown by teratoma formation. Directed differentiation of these clones to neutrophils, hepatocytes or cardiomyocytes was not hindered by the knock-in of marker genes into the AAVS1 sites. Notably, transgene expression was stable in undifferentiated RhiPSCs and differentiated cell types derived from the RhiPSC (Figure 1), in contrast to prior experience with viral vector delivery. We have established a computational platform to assess off-target effects of guide RNAs in the rhesus genome. Genetically marked RhiPSCs afford a unique opportunity to develop clinically relevant models for iPSC-based cell therapies.



**Figure 1** Stable transgene expression in CRISPR edited clones after *in vitro* and *in vivo* differentiation

RhiPSC-hΔCD19-derived cells maintained strong expression of hΔCD19 after *in vitro* spontaneous differentiation (15 days) and *in vivo* teratoma formation (6-8 weeks).

**Table 1** Summary of CRISPR-mediated gene editing in rhesus iPSCs

Original iPSC clone	Reporter gene	Clones with TI/Clones screened <sup>1</sup>	Clones without RI/Clones with TI <sup>2</sup>
ZG15-M11-10	hΔCD19	4/4	2/8
	GFP	14/14	5/9
ZG32-3-4	hΔCD19	ND	1/4
	GFP	ND	2/4
ZH26-HS41	hΔCD19	ND	1/4
Total		18/18 (100%)	11/29 (37.9%)

RI: random integration, TI: targeted integration, ND: not determined  
<sup>1</sup>based on by PCR analysis <sup>2</sup>based on Southern blot analysis

## 528. Towards Personalized Cell Therapy for Cancer: Tumor-Homing Human Induced Neural Stem Cells

Juli Bago<sup>1</sup>, Onyi Okolie<sup>1</sup>, Raluca Dumitru<sup>2</sup>, Matt Ewend<sup>3</sup>, Shawn Hingtgen<sup>1</sup>

<sup>1</sup>Eshelman School of Pharmacy, The University of North Carolina at Chapel Hill, Chapel Hill, NC, <sup>2</sup>UNC School of Medicine, The University of North Carolina at Chapel Hill, Chapel Hill, NC, <sup>3</sup>UNC Department of Neurosurgery, The University of North Carolina at Chapel Hill, Chapel Hill, NC

**Background:** Engineered neural stem cells (NSC) are a promising new approach to treating glioblastoma (GBM). In clinical trials, the ideal NSC drug carrier should be easily isolated and autologous to avoid immune rejection. **Methods:** As a new approach to personalized NSC therapy for cancer, we directly transdifferentiated (TD) human fibroblasts in induced neural stem cells (h-iNSCs). The h-iNSCs were engineered to express optical reporters and either the pro-apoptotic agent TRAIL or thymidine kinase. The tumor-homing migration and therapeutic efficacy of cytotoxic h-iNSCs were then assessed in human-derived GBM models of solid and surgically resected disease. All statistical tests were two-sided. **Results:** Our new single-factor Sox2 strategy converted human skin fibroblasts into nestin+ h-iNSCs in only 4 days and the h-iNSCs survived in the brain of mice for 3 weeks. Time-lapse motion analysis showed h-iNSCs rapidly migrated to human GBMs cells and penetrated solid human GBM spheroids. h-iNSC delivery of TRAIL reduced solid human GBM xenografts 250-fold in 3 weeks and prolonged median survival from 22 to 49 days ( $P < 0.01$ ). h-iNSC prodrug/enzyme therapy regressed patient-derived GBM xenografts 20-fold and extended survival from 32 to 62 days ( $P < 0.01$ ). Mimicking clinical NSC therapy, intra-cavity h-iNSC thymidine kinase/ganciclovir therapy delayed the regrowth of post-surgical GBMs 3-fold and prolonged survival in mice from 46 to 60 days. **Conclusions:** Transdifferentiating human skin into h-iNSCs is a new platform for creating tumor-homing cytotoxic cell therapies for cancer. Translating this approach has the potential to avoid carrier rejection and maximize treatment durability in patient trials.

## RNA Virus Vectors

### 529. Lentiviral Vectors with a Reduced Splicing Interference Potential Have a Significantly Improved Safety Profile *In Vivo*

Daniela Cesana<sup>1</sup>, Pierangela Gallina<sup>1</sup>, Laura Rudilosso<sup>1</sup>, Andrea Calabria<sup>1</sup>, Giulio Spinozzi<sup>1</sup>, Ivan Merelli<sup>2</sup>, Luciano Milanese<sup>2</sup>, Eugenio Montini<sup>1</sup>

<sup>1</sup>San Raffaele- Telethon Institute for Gene Therapy, Milan, Italy,

<sup>2</sup>Italian National Research Council, Institute of Biomedical Technologies, Milan, Italy

Genotoxicity assays based on systemic vector injection into newborn tumor-prone *Cdkn2a*<sup>-/-</sup> and *Cdkn2a*<sup>+/-</sup> mice has shown that self-inactivating (SIN) lentiviral vector (LV) harboring strong or moderate enhancer/promoters in internal position caused acceleration in hematopoietic tumor onset compared to control mice. Integration site (IS) analysis in vector-induced tumors showed that oncogene activation or tumor suppressor inactivation occurs by mechanisms of aberrant splicing and/or enhancer-mediated overexpression of cellular genes. Although oncogene activation may be reduced by the use of SIN design, moderate cellular promoters and insulator sequences, how to reduce genotoxic splicing-capture events and aberrant transcript formation triggered by vector integration is still unclear. Here, we specifically designed SINLVs harboring sequences complementary to microRNAs (mirT sequence) which are active in hematopoietic cells (mir223 and mir142-3p) within the SIN LTR (mirT-LTR.LV)

or in the vector backbone and outside the gene expression cassette (mirT-LV). In our rationale, the mirT sequences when incorporated in an aberrantly generated mRNA would be selectively degraded through the miRNA pathway. Thus, by taking advantage of our *in vivo* models, we assessed the genotoxicity of these LVs with mirT sequences. Systemic injection of mirsT-LTR.LV (N=34) and mirT-LV (N=39) in *Cdkn2a*<sup>-/-</sup> mice did not cause any significant acceleration in hematopoietic tumor onset compared to un-injected mice (N=37) or mice injected with a SINLV that does not harbor mirT sequences (N=24). Similar results have been obtained after injection of the same vectors in *Cdkn2a*<sup>+/-</sup> mice (N=29 mirsT-LTR.LV, N=25 mirT-LV, N=40 un-injected and N=15 injected control mice). To gain additional information on the safety profile of these vectors, we performed IS analysis (N>10,000) in tumor-derived DNA. By this analysis, we previously found that *Map3k8* activation by LV insertions was the major mechanism of genotoxicity when prototypical SINLVs were injected into *Cdkn2a*<sup>-/-</sup> mice. Now, we found that mice treated with mirsT-LTR.LV and mirT-LV did not show any *Map3k8* activating insertions, suggesting that the new vectors are efficient in preventing its activation and confirming their superior safety profile. Furthermore, as expected, *Pten* was the most frequently targeted gene in tumors derived from *Cdkn2a*<sup>-/-</sup> mice injected with the LVs harboring mirT sequences. *Pten* insertions mainly targeted exons, suggesting the potential inactivation of its transcription unit. Finally, we found that *Sfi1* was the major Common Insertion Site (CIS) in *Cdkn2a*<sup>+/-</sup> mice injected with LVs harboring mirT sequences. This CIS gene however appears to be the product of an intrinsic bias of LV integration, rather than the result of a selection process. Overall, our studies showed that these new advanced design LVs have a significantly improved safety profile and could represent the vector design of choice in future gene therapy applications.

### 530. Lentiviral Vector Particles Pseudotyped with Wild-Type Baboon Endogenous Retrovirus (BAEV) Glycoprotein Outperform VSV-G Particles in Transducing Human CD34+ Cells Isolated from Cytokine-Mobilized Peripheral Blood or Bone Marrow

Phillip Hargrove, Yoon-Sang Kim, Matthew Wielgosz, Arthur W. Nienhuis  
Hematology, St. Jude Children's Research Hospital, Memphis, TN

Lentiviral vector gene therapy for hematopoietic disorders caused by single gene mutation or deficiency has demonstrated success in clinical trials. However, efficient gene delivery is still challenging, requiring high multiplicity of infection (MOI) to achieve average vector copy numbers of at least 1 per cell. Conditions utilizing high MOI result in improved transduction rates and adequate copy number but these benefits can coincide with potential insertional mutagenesis. Attempting to achieve optimal gene transfer at reduced MOI, we directly compared self-inactivating (SIN) lentiviral vector particles encoding eGFP under control of a murine stem cell virus (MSCV) promoter/enhancer pseudotyped with envelope glycoproteins for BaEV or vesicular stomatitis virus (VSV). BaEV proteins were either full-length (BaWT) or lacked the terminal R-peptide (BaR-less), a version previously reported to improve infectious titer (TU, transducing units per mL) using transient production procedures. Using a standardized four-plasmid transient production protocol, cells transfected with R-less expression plasmids produced syncytia; an issue that resolved using BaWT. Titers were significantly higher for virus packaged with BaWT compared to R-less (BaR-less:  $3.6 \times 10^5 \pm 6.6 \times 10^4$  N=12; BaWT  $2.4 \times 10^6 \pm 4.5 \times 10^5$ ; n=10; p<0.001) determined by flow cytometry analysis of GFP expression in transduced HEK-293T cells. However, these values were 10- to 20-fold less than those observed for VSV-G ( $3.5 \times 10^7 \pm 4.5 \times 10^6$ ).

Human CD34+ hematopoietic stem/progenitor cells isolated from bone marrow (BM) or cytokine-mobilized peripheral blood (mPB) of healthy donors were prestimulated and transduced overnight on retronectin-coated plates with BaWT particles at an MOI of 0.5, 1, 2, or 4. The following day, cells were either plated in methylcellulose to assess colony-formation (CFU), maintained in liquid culture (Bulk), or transplanted into NOD-*scid* IL2Rg<sup>null</sup> (NSG) mice pre-conditioned with busulfan (n=10 mice/1x10<sup>6</sup> cells each). Gene transfer efficiency was gauged by expression of GFP following flow cytometry analysis of cells maintained in culture or visual inspection of colonies growing in methylcellulose using an inverted fluorescence microscope after 6 or 12 days, respectively. Transduction efficiency increased with viral MOI reaching peak levels using an MOI of 2 (Bulk, 93% GFP+; CFU, 98% GFP+). Six NSG mice survived to 14 weeks post-transplant and demonstrated engraftment of CD45+ cells ranging from 19 to 54% ( $39 \pm 13\%$ ; mean  $\pm$  SD) and GFP marking ranging from 32 to 59% ( $41 \pm 10\%$ ) determined by flow cytometry. Finally, we compared GFP-encoding particles pseudotyped with VSV-G or BaWT normalizing for levels of p24 quantified by ELISA (BaWT, 1155.0 pg/ml,  $3.3 \times 10^6$  TU; VSV-G, 1164.9 pg/ml,  $5.1 \times 10^7$  TU) to account for differences in calculated titer. Prestimulated mPB CD34+ cells were transduced overnight and placed into methylcellulose or transplanted into 15 NSG mice each. Methylcellulose colonies were analyzed for GFP after 12 days of growth (BaWT, 95.6%; VSV-G, 76.6%). Transplanted mice will be analyzed at 16-18 weeks post-transplant to measure engraftment and GFP expression. We believe the stability of producer cells expressing BaWT, the high efficiency of transduction at low MOI, and the ability to transduce adequate numbers of cells with unconcentrated virus supernatant warrant continued optimization of transient production methods and development of a stable producer cell line utilizing BaWT envelope as an alternative to VSV-g.

### 531. Computational Pipeline for the Identification of Integration Sites and Novel Method for the Quantification of Clone Sizes in Clonal Tracking Studies

Lorena Leonardelli<sup>1</sup>, Danilo Pellin<sup>2</sup>, Serena Scala<sup>1</sup>, Francesca Dionisio<sup>1</sup>, Luca Basso Ricci<sup>1</sup>, Davide Cittaro<sup>3</sup>, Clelia Di Serio<sup>2</sup>, Alessandro Aiuti<sup>1</sup>, Luca Biasco<sup>1</sup>  
<sup>1</sup>San Raffaele Telethon Institute for Gene Therapy (TIGET), Milan, Italy, <sup>2</sup>CUSSB, Vita-Salute University, Milan, Italy, <sup>3</sup>Center for Translational Genomics and Bioinformatics, San Raffaele Scientific Institute, Milan, Italy

Gene-corrected cells in Gene Therapy (GT) treated patients can be tracked *in vivo* by means of vector integration site (IS) analysis, since each engineered clone becomes univocally and stably marked by an individual IS. As the proper IS identification and quantification is crucial to accurately perform clonal tracking studies, we designed a customizable and tailored pipeline to analyze LAM-PCR amplicons sequenced by Illumina MiSeq/HiSeq technology. The sequencing data are initially processed through a series of quality filters and cleaned from vector and Linker Cassette (LC) sequences with customizable settings. Demultiplexing is then performed according to the recognition of specific barcodes combination used upon library preparation and the sequences are aligned to the reference genome. Importantly, the human genome assembly Hg19 is composed of 93 contigs, among which the mitochondrial genome, unlocalized and unplaced contigs and some alternative haplotypes of chr6. While previous approaches aligned IS sequences only to the standard 24 human chromosomes, using the whole assembled genome allowed improving alignment accuracy and concomitantly increased the amount of detectable ISs. To date, we have processed 28 independent human sample sets retrieving 260,994 ISs from 189,270,566 sequencing reads. Although, sequencing read counts at each IS have